

See discussions, stats, and author profiles for this publication at: <https://www.researchgate.net/publication/278324583>

# Stable Phase Equilibrium of Aqueous Quaternary System $\text{Li}^+$ , $\text{K}^+$ , $\text{Mg}^{2+}$ // Borate– $\text{H}_2\text{O}$ at 348 K

ARTICLE in JOURNAL OF CHEMICAL & ENGINEERING DATA · DECEMBER 2014

Impact Factor: 2.04 · DOI: 10.1021/je5008108

---

READS

12

5 AUTHORS, INCLUDING:



Ying Zeng

Chengdu University of Technology

45 PUBLICATIONS 243 CITATIONS

SEE PROFILE

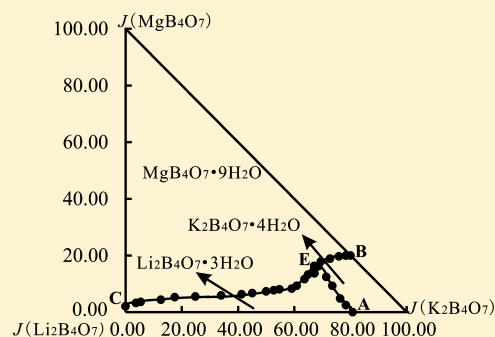
# Stable Phase Equilibrium of Aqueous Quaternary System $\text{Li}^+$ , $\text{K}^+$ , $\text{Mg}^{2+}$ //Borate– $\text{H}_2\text{O}$ at 348 K

Qi Tan,<sup>†</sup> Ying Zeng,<sup>\*,†,‡</sup> Pengtao Mu,<sup>†</sup> Xudong Yu,<sup>†</sup> and Yujuan Zhang<sup>†</sup>

<sup>†</sup>College of Materials and Chemistry & Chemical Engineering, Chengdu University of Technology, Chengdu 610059, People's Republic of China

<sup>‡</sup>Mineral Resources Chemistry Key Laboratory of the Higher Education Institutions of Sichuan Province, Chengdu 610059, People's Republic of China

**ABSTRACT:** The solubility values and physicochemical properties such as densities, refractive indices, and pH values of the equilibrium solution in the quaternary system  $\text{Li}^+$ ,  $\text{K}^+$ ,  $\text{Mg}^{2+}$ //borate– $\text{H}_2\text{O}$  at 348 K were measured by isothermal dissolution method. The phase diagram, water content diagram, and the diagrams of the physicochemical properties versus composition were constructed using the measured data. Results show that this quaternary system at 348 K is of a simple type, no double salt or solid solution formed. The stable phase diagram of this quaternary system consists of one invariant point, three univariant curves, and three crystalline phase areas. The invariant point saturated with three salts corresponding to lithium tetraborate trihydrate ( $\text{Li}_2\text{B}_4\text{O}_7 \cdot 3\text{H}_2\text{O}$ ), potassium tetraborate tetrahydrate ( $\text{K}_2\text{B}_4\text{O}_7 \cdot 4\text{H}_2\text{O}$ ), and hungchaoite ( $\text{MgB}_4\text{O}_7 \cdot 9\text{H}_2\text{O}$ ). The crystallization field of  $\text{MgB}_4\text{O}_7 \cdot 9\text{H}_2\text{O}$  is the maximum, meaning that the salt magnesium borate has the smallest solubility among the coexisting salts. Comparisons between the stable phase diagrams at 288 K and 348 K show that the crystallization zones of  $\text{MgB}_4\text{O}_7 \cdot 9\text{H}_2\text{O}$  decreased at 348 K, while the crystallization zones of  $\text{K}_2\text{B}_4\text{O}_7 \cdot 4\text{H}_2\text{O}$  and  $\text{Li}_2\text{B}_4\text{O}_7 \cdot 3\text{H}_2\text{O}$  both enlarged at 348 K. On the univariant curve CE, the water contents decrease with the increase of  $J(\text{K}_2\text{B}_4\text{O}_7)$ ; the densities and refractive indices both increase with the increase of  $J(\text{K}_2\text{B}_4\text{O}_7)$  and reach the maximum at invariant point E.



## INTRODUCTION

Brine, including salt lake brine and underground brine, is an important mineral resource. Pingluo underground brine, located in the west of Sichuan Basin, is well-known for being rich in potassium, lithium, and borate.<sup>1</sup> The content of potassium is as high as 53.27 g·L<sup>-1</sup>, which is much higher than other famous salt lake brines such as Qarhan Salt Lake brine (15 g·L<sup>-1</sup>)<sup>2</sup> and Atacama Salt Lake brine (23.6 g·L<sup>-1</sup>).<sup>3</sup> The content of boron in the brine is up to 4.99 g·L<sup>-1</sup>, nearly 32 times of the industrial grade for comprehensive utilization. The content of lithium is also much higher than the industry mined grade.<sup>4</sup> Thus, there is vast developing prospective for the Pingluo underground brine.

The thermodynamic investigation of the phase diagrams of the solid–liquid system plays an important role in exploiting brine resources and also in describing the geochemistry evolution of brine minerals. Pingluo underground brine is a complex water–salt coexisting system; the main components of the brine are sodium, potassium, magnesium, lithium, rubidium and chloride, and borate, etc.<sup>5</sup> When the sodium chloride is separated by crystallization in the process of evaporation, the main composition of Pingluo underground brine can be simplified as a six-component system  $\text{Li}^+$ ,  $\text{K}^+$ ,  $\text{Rb}^+$ ,  $\text{Mg}^{2+}$ // $\text{Cl}^-$ , borate– $\text{H}_2\text{O}$ .<sup>6</sup> The Pingluo underground brine is deeply buried in the ground (over 4500 m), and the temperature of the brine is up to 393 K.<sup>4</sup> In the mining process, the

temperature of the brine decreased gradually. Therefore, the thermodynamics stable phase equilibria research focus on different temperature is necessary. So far, a series of phase equilibria studies focused on the subsystem of Pingluo underground brine at different temperatures has been done by our group, such as the ternary system  $\text{K}^+$ ,  $\text{Mg}^{2+}$ // $\text{Cl}^-$ – $\text{H}_2\text{O}$  and  $\text{K}^+$ ,  $\text{Rb}^+$ // $\text{Cl}^-$ – $\text{H}_2\text{O}$  at 298 K,<sup>7</sup> 323 K,<sup>8</sup> and 348 K;<sup>9</sup> the quaternary system  $\text{Li}^+$ ,  $\text{K}^+$ ,  $\text{Rb}^+$ // $\text{Cl}^-$ – $\text{H}_2\text{O}$  at 298 K,<sup>10</sup> 323 K,<sup>11</sup> and 348 K;<sup>12</sup> and the quaternary system  $\text{Li}^+$ ,  $\text{K}^+$ ,  $\text{Mg}^{2+}$ // $\text{Cl}^-$ – $\text{H}_2\text{O}$  at 323 K.<sup>13</sup> The aqueous quaternary system  $\text{Li}^+$ ,  $\text{K}^+$ ,  $\text{Mg}^{2+}$ //borate– $\text{H}_2\text{O}$  is one of the most important subsystems of the complex multiple systems mentioned previously. The stable phase equilibrium of this quaternary system at 288 K has been studied by Xiao et al.;<sup>14</sup> results show that the stable phase diagram of this quaternary system at 288 K consists of three single salt crystallization fields corresponding to  $\text{Li}_2\text{B}_4\text{O}_7 \cdot 3\text{H}_2\text{O}$ ,  $\text{K}_2\text{B}_4\text{O}_7 \cdot 4\text{H}_2\text{O}$ , and  $\text{MgB}_4\text{O}_7 \cdot 9\text{H}_2\text{O}$ . In order to figure out the effect of temperature on this quaternary system and provide basic data for the development of underground brine, research focused on the stable phase equilibrium of the system  $\text{Li}^+$ ,  $\text{K}^+$ ,  $\text{Mg}^{2+}$ //borate– $\text{H}_2\text{O}$  at different temperature is necessary.

Received: September 3, 2014

Accepted: November 13, 2014

Published: December 1, 2014

Table 1. Solubility and Analytical Experimental Reagents

| chemical name  | source                                  | mass fraction purity |
|--|---|----------------------|
| potassium tetraborate ( $\text{K}_2\text{B}_4\text{O}_7 \cdot 5\text{H}_2\text{O}$ ) | Chengdu Kelong Chemical Reagent Plant   | 0.995                |
| lithium tetraborate ( $\text{Li}_2\text{B}_4\text{O}_7$ )                            | Chengdu Kelong Chemical Reagent Plant   | 0.995                |
| Hungchaoite ( $\text{MgB}_4\text{O}_5(\text{OH})_4 \cdot 7\text{H}_2\text{O}$ )      | synthesized in laboratory <sup>17</sup> | 0.990                |
| sodium tetraphenylboron (STPB)   | Chengdu Kelong Chemical Reagent Plant   | 0.990                |
| cetyltrimethylammonium bromide (CTAB)  | Chengdu Kelong Chemical Reagent Plant   | 0.990                |
| ethylenediamine tetraacetic acid disodium salt (EDTA)                                | Chengdu Kelong Chemical Reagent Plant   | 0.990                |

Table 2. Experimental Values of Densities, Refractive Indices, pH Value and Solubility of the Equilibrium Solution in the Quaternary System  $\text{Li}^+$ ,  $\text{K}^+$ ,  $\text{Mg}^{2+}$ //Borate– $\text{H}_2\text{O}$  at 348 K and Pressure  $p = 0.1 \text{ MPa}^a$ 

| no. | density                             | refractive index | pH value | $w(\text{B}) \times 100$    |                                      |                                     |                         | Jänecke index of dry salt $J(\text{MgB}_4\text{O}_7) + J(\text{Li}_2\text{B}_4\text{O}_7) + J(\text{K}_2\text{B}_4\text{O}_7) = 100$ |                                      |                                     |                         | solid phase  |
|-----|-------------------------------------|------------------|----------|-----------------------------|--------------------------------------|-------------------------------------|-------------------------|--|--------------------------------------|-------------------------------------|-------------------------|--------------|
|     | ( $\text{g} \cdot \text{cm}^{-3}$ ) |                  |          | $w(\text{MgB}_4\text{O}_7)$ | $w(\text{Li}_2\text{B}_4\text{O}_7)$ | $w(\text{K}_2\text{B}_4\text{O}_7)$ | $w(\text{H}_2\text{O})$ | $J(\text{MgB}_4\text{O}_7)$  | $J(\text{Li}_2\text{B}_4\text{O}_7)$ | $J(\text{K}_2\text{B}_4\text{O}_7)$ | $J(\text{H}_2\text{O})$ |              |
| 1A  | 1.5628                              | 1.3892           | 9.84     | 0.00                        | 6.33                                 | 36.71                               | 56.96                   | 0.00   | 19.23                                | 80.77                               | 1624                    | LB + KB      |
| 2   | 1.5466                              | 1.4035           | 9.82     | 0.91                        | 6.58                                 | 37.25                               | 55.26                   | 2.49   | 19.11                                | 78.40                               | 1507                    | LB + KB      |
| 3   | 1.5635                              | 1.4055           | 9.67     | 1.87                        | 6.87                                 | 38.43                               | 52.83                   | 4.83   | 18.84                                | 76.33                               | 1359                    | LB + KB      |
| 4   | 1.5709                              | 1.4110           | 9.57     | 4.09                        | 7.10                                 | 41.97                               | 46.84                   | 9.31   | 17.17                                | 73.52                               | 1063                    | LB + KB      |
| 5   | 1.5962                              | 1.4195           | 9.46     | 5.59                        | 6.84                                 | 41.64                               | 45.93                   | 12.46  | 16.18                                | 71.36                               | 1020                    | LB + KB      |
| 6E  | 1.6077                              | 1.4230           | 9.30     | 7.31                        | 6.44                                 | 40.19                               | 46.06                   | 16.22  | 15.17                                | 68.60                               | 1019                    | LB + MB + KB |
| 7B  | 1.5634                              | 1.4128           | 8.99     | 8.11                        | 0.00                                 | 42.28                               | 49.61                   | 19.96  | 0.00                                 | 80.04                               | 1217                    | MB + KB      |
| 8   | 1.5689                              | 1.4130           | 9.04     | 7.54                        | 0.63                                 | 38.56                               | 53.27                   | 19.91  | 1.77                                 | 78.32                               | 1402                    | MB + KB      |
| 9   | 1.5700                              | 1.4135           | 9.13     | 7.69                        | 1.62                                 | 38.49                               | 52.20                   | 19.71  | 4.41                                 | 75.88                               | 1333                    | MB + KB      |
| 10  | 1.5748                              | 1.4192           | 9.20     | 7.66                        | 3.21                                 | 38.45                               | 50.68                   | 18.85  | 8.39                                 | 72.77                               | 1242                    | MB + KB      |
| 11  | 1.5883                              | 1.4225           | 9.22     | 7.60                        | 5.06                                 | 38.43                               | 48.91                   | 17.87  | 12.63                                | 69.50                               | 1146                    | MB + KB      |
| 12E | 1.6077                              | 1.4230           | 9.30     | 7.31                        | 6.44                                 | 40.19                               | 46.06                   | 16.22  | 15.17                                | 68.60                               | 1019                    | LB + MB + KB |
| 13C | 1.1248                              | 1.3381           | 7.82     | 0.12                        | 5.26                                 | 0.00                                | 94.62                   | 2.10   | 97.90                                | 0.00                                | 16527                   | LB + MB      |
| 14  | 1.1251                              | 1.3400           | 7.84     | 0.20                        | 5.39                                 | 0.29                                | 94.12                   | 3.25   | 93.12                                | 3.63                                | 15260                   | LB + MB      |
| 15  | 1.1262                              | 1.3405           | 7.87     | 0.29                        | 6.84                                 | 0.56                                | 92.31                   | 3.63   | 90.97                                | 5.40                                | 11522                   | LB + MB      |
| 16  | 1.1361                              | 1.3405           | 7.92     | 0.39                        | 7.01                                 | 1.46                                | 91.14                   | 4.35   | 83.11                                | 12.54                               | 10141                   | LB + MB      |
| 17  | 1.1422                              | 1.3415           | 8.01     | 0.52                        | 7.21                                 | 2.26                                | 90.01                   | 5.25   | 77.22                                | 17.54                               | 9047                    | LB + MB      |
| 18  | 1.1541                              | 1.3426           | 8.09     | 0.65                        | 7.37                                 | 3.64                                | 88.34                   | 5.77   | 69.40                                | 24.83                               | 7807                    | LB + MB      |
| 19  | 1.1601                              | 1.3435           | 8.17     | 0.79                        | 7.48                                 | 5.84                                | 85.89                   | 5.97   | 60.06                                | 33.97                               | 6472                    | LB + MB      |
| 20  | 1.2086                              | 1.3467           | 8.26     | 0.96                        | 7.42                                 | 8.07                                | 83.55                   | 6.38   | 52.36                                | 41.26                               | 5533                    | LB + MB      |
| 21  | 1.2671                              | 1.3478           | 8.31     | 1.06                        | 7.13                                 | 9.20                                | 82.61                   | 6.75   | 48.20                                | 45.05                               | 5241                    | LB + MB      |
| 22  | 1.2804                              | 1.3497           | 8.37     | 1.31                        | 7.14                                 | 11.56                               | 79.99                   | 7.37   | 42.63                                | 50.00                               | 4482                    | LB + MB      |
| 23  | 1.3041                              | 1.3538           | 8.49     | 1.47                        | 7.08                                 | 13.02                               | 78.43                   | 7.74   | 39.56                                | 52.70                               | 4113                    | LB + MB      |
| 24  | 1.3553                              | 1.3596           | 8.59     | 1.59                        | 6.88                                 | 13.97                               | 77.56                   | 8.10   | 37.19                                | 54.71                               | 3935                    | LB + MB      |
| 25  | 1.3896                              | 1.3621           | 8.66     | 1.82                        | 6.72                                 | 16.88                               | 74.58                   | 8.30   | 32.52                                | 59.18                               | 3387                    | LB + MB      |
| 26  | 1.4566                              | 1.3785           | 8.72     | 2.15                        | 6.48                                 | 18.27                               | 73.10                   | 9.31   | 29.81                                | 60.88                               | 3156                    | LB + MB      |
| 27  | 1.4859                              | 1.3830           | 8.87     | 3.17                        | 6.41                                 | 22.47                               | 67.95                   | 11.63  | 24.97                                | 63.40                               | 2484                    | LB + MB      |
| 28  | 1.5202                              | 1.3917           | 8.91     | 4.14                        | 6.43                                 | 26.37                               | 63.06                   | 13.25  | 21.85                                | 64.91                               | 2011                    | LB + MB      |
| 29  | 1.5533                              | 1.4019           | 9.14     | 4.93                        | 6.48                                 | 31.44                               | 57.15                   | 13.70  | 19.11                                | 67.19                               | 1582                    | LB + MB      |
| 30  | 1.5901                              | 1.4206           | 9.21     | 6.60                        | 6.34                                 | 35.37                               | 51.69                   | 16.28  | 16.61                                | 67.11                               | 1271                    | LB + MB      |
| 31E | 1.6077                              | 1.4230           | 9.30     | 7.31                        | 6.44                                 | 40.19                               | 46.06                   | 16.22  | 15.17                                | 68.60                               | 1019                    | LB + MB + KB |

<sup>a</sup>Standard uncertainties  $u$  are as follows:  $u(T) = 0.50 \text{ K}$ ;  $u_c(p) = 0.05$ ;  $u_c(\rho) = 2.0 \times 10^{-4}$ ;  $u_c(n) = 1.0 \times 10^{-4}$ ;  $u_c(\text{pH}) = 0.02$ ;  $u_c(\text{Li}_2\text{B}_4\text{O}_7) = 0.0050$ ;  $u_c(\text{K}_2\text{B}_4\text{O}_7) = 0.0050$ ;  $u_c(\text{MgB}_4\text{O}_7) = 0.0050$ ;  $w(\text{B})$ , mass fraction of B;  $J(\text{B})$ , the Jänecke index values of B; LB,  $\text{Li}_2\text{B}_4\text{O}_7 \cdot 3\text{H}_2\text{O}$ ; MB,  $\text{MgB}_4\text{O}_7 \cdot 9\text{H}_2\text{O}$ ; KB,  $\text{K}_2\text{B}_4\text{O}_7 \cdot 4\text{H}_2\text{O}$ .

The quaternary system  $\text{Li}^+$ ,  $\text{K}^+$ ,  $\text{Mg}^{2+}$ //borate– $\text{H}_2\text{O}$  consists of three ternary subsystems. In our previous research, the phase equilibria of its ternary subsystems  $\text{Li}^+$ ,  $\text{K}^+$ //borate– $\text{H}_2\text{O}$ <sup>15</sup> and  $\text{K}^+$ ,  $\text{Mg}^{2+}$ //borate– $\text{H}_2\text{O}$ <sup>16</sup> at 348 K have been studied. Results show that these two ternary systems at 348 K are all of simple type, no double salt or solid solution formed. This work is a continuation of our previous research. Up to now, no report has been found about the stable phase equilibrium of the aqueous quaternary system  $\text{Li}^+$ ,  $\text{K}^+$ ,  $\text{Mg}^{2+}$ //borate– $\text{H}_2\text{O}$  at 348 K. Therefore, the solubility values and physicochemical properties such as densities, refractive indices, and pH values of the equilibrium solution are presented in this work.

Meanwhile, the comparisons between the stable phase diagrams at 288 and 348 K are made in this work.

## EXPERIMENTAL SECTION

**Reagents and Apparatus.** The inorganic chemicals used in this study were all analytical purity grade and tabulated in Table 1. Deionized water, used in the experiments, has an electrical conductivity less than  $1 \times 10^{-4} \text{ s} \cdot \text{m}^{-1}$  and  $\text{pH} \approx 6.60$ .

A THZ-82 type digital display constant temperature water bath kettle (Jintan Guosheng Experimental Instrument Manufactory, China) was used for the stable phase equilibrium experiments. The temperature precision was  $\pm 0.5 \text{ K}$ . A

standard analytical balance of 110 g capacity and 0.0001 g resolution (type AL104, Mettler Toledo Instruments Co., Ltd.) was employed to determine the weight of samples. A WYA type Abbe refractometer, conducted in a thermostat at  $(348 \pm 0.5)$  K, was used for measuring the refractive index of the equilibrated solution with a precision of 0.0001. All pH values were measured with pH-25 type pH meter at  $(348 \pm 0.5)$  K. An inductively coupled plasma optical emission spectrometer (type 5300 V, PerkinElmer Instrument Corp. of America) was employed to determine the lithium ion concentrations in solution. An X-ray diffraction analyzer (DX-2700 with Cu  $K\alpha$  radiation) was used to analyze the phase composition of solid salt.

**Analytical Methods.** The  $\text{Li}^+$  composition was analyzed by inductively coupled plasma optical emission spectrometry (precision, less than 0.5 mass %, type ICP-OES 5300 V). The amount of  $\text{K}^+$  was analyzed by sodium tetraphenylborate–hexadecyl trimethylammonium bromide (STPB–CTAB) back-titration with a precision of  $\pm 0.5$  %; The  $\text{Mg}^{2+}$  concentration was determined by titration with ethylenediamine tetraacetic acid (EDTA) stand solution in the presence of indicator of K–B with a precision of  $\pm 0.5$  %. The composition of borate was measured by alkalimetry in the presence of mannitol (precision,  $\pm 0.5$  %).<sup>18</sup> Every sample was analyzed 3 times in parallel; the precision was calculated as the following equation.

$$\text{precision}/\% = \frac{V_{\text{exp}} - V_{\text{av}}}{V_{\text{av}}} \times 100 \quad (1)$$

where,  $V_{\text{exp}}$  is the experimental data;  $V_{\text{av}}$  is the average data of the parallel samples. Each analysis was repeated three times with triplicate samples prepared for each data point, and the average value of three measurements was considered as the final value of the analysis.

**Experimental Method.** The stable phase equilibrium of the quaternary system was investigated at 348 K using an isothermal dissolution method.<sup>19</sup> The third component was added gradually from the invariant point of the ternary system at the same temperature to obtain the system points. For instance, from the invariant point of system  $\text{K}^+$ ,  $\text{Mg}^{2+}$ //borate– $\text{H}_2\text{O}$  at 348 K,  $\text{Li}_2\text{B}_4\text{O}_7$  was added gradually for obtaining the system points. All of the artificial brine samples were put into the tightly sealed glass bottles, and these bottles were placed in the constant temperature water bath kettle with the temperature  $((348 \pm 0.5)$  K) and a constant oscillation frequency (120 rpm) to achieve a balance. During the equilibrium process, the supernatant phase was taken for chemical analysis periodically, when the composition of the supernatant phase remained constant, the dissolution equilibrium was reached. Experimental results show that in order to accelerate equilibration, the artificial brine samples need a constant oscillation frequency (120 rpm) for more than 4 weeks at  $(348 \pm 0.5)$  K. After reaching equilibrium, the liquid and solid phases were separated by suction filtration at  $(348 \pm 0.5)$  K. The composition of solution were measured by chemical analysis; the densities of the liquid samples were measured with the specific gravity bottle method with a precision of  $\pm 0.0002$  g·cm<sup>−3</sup>; the refractive indices of equilibrated liquid phase were determined by Abbe refractometer, which was conducted in a thermostat at  $(348 \pm 0.5)$  K. The equilibrium solid samples were dried at 348 K and identified by the powder X-ray diffraction method.

## RESULTS AND DISCUSSION

The experimental results, including the solubility values, densities, refractive indices, pH values, and the chemical composition of equilibrium solids for the quaternary system  $\text{Li}^+$ ,  $\text{K}^+$ ,  $\text{Mg}^{2+}$ //borate– $\text{H}_2\text{O}$  at 348 K are listed in Table 2. The ion concentration values of the stable equilibrium solutions are expressed in mass fraction  $w(\text{B})$  (with  $w(\text{Li}_2\text{B}_4\text{O}_7) + w(\text{K}_2\text{B}_4\text{O}_7) + w(\text{MgB}_4\text{O}_7) + w(\text{H}_2\text{O}) = 1$ ) and Jänecke index  $J(\text{B})$  (with  $J(\text{Li}_2\text{B}_4\text{O}_7) + J(\text{K}_2\text{B}_4\text{O}_7) + J(\text{MgB}_4\text{O}_7) = 100$ ), where B represents  $\text{MgB}_4\text{O}_7$ ,  $\text{Li}_2\text{B}_4\text{O}_7$ ,  $\text{K}_2\text{B}_4\text{O}_7$ , or  $\text{H}_2\text{O}$ . The Jänecke index  $J(\text{B})$  is a dry salt mole percentage and can be calculated with the following correlations.

$$[\text{M}] = \frac{w(\text{Li}_2\text{B}_4\text{O}_7)}{169.12} + \frac{w(\text{K}_2\text{B}_4\text{O}_7)}{233.44} + \frac{w(\text{MgB}_4\text{O}_7)}{179.55} \quad (2)$$

$$J(\text{K}_2\text{B}_4\text{O}_7) = \frac{w(\text{K}_2\text{B}_4\text{O}_7)}{233.44[\text{M}]} \times 100 \quad (3)$$

$$J(\text{H}_2\text{O}) = \frac{w(\text{H}_2\text{O})}{18.02[\text{M}]} \times 100 \quad (4)$$

Based on the experimental data in Table 2, the phase diagram of the quaternary system  $\text{Li}^+$ ,  $\text{K}^+$ ,  $\text{Mg}^{2+}$ //borate– $\text{H}_2\text{O}$  at 348 K was constructed in Figure 1. In Figure 1, points A, B, and C are

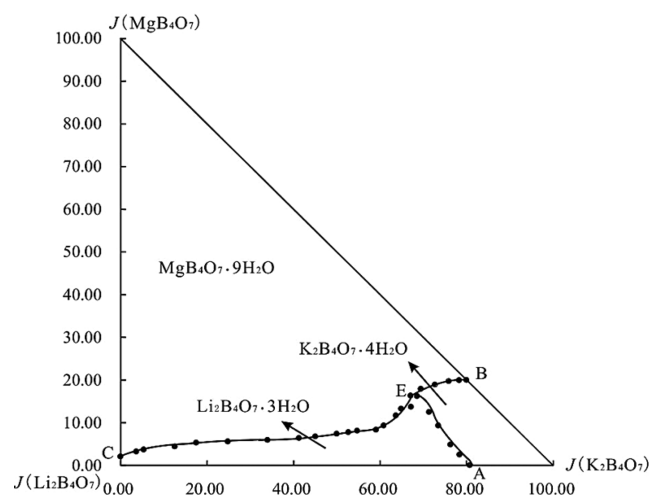


**Figure 1.** Phase diagram of the quaternary system  $\text{Li}^+$ ,  $\text{K}^+$ ,  $\text{Mg}^{2+}$ //borate– $\text{H}_2\text{O}$  at 348 K.

the invariant points of three ternary subsystems and point E is the invariant point of the quaternary system. Figure 2 shows the comparison of the stable phase diagrams of this quaternary system at 288 K<sup>14</sup> and 348 K. The crystallization forms of the solid phase were confirmed with an X-ray diffraction analysis method and demonstrated in Figure 3.

As shown in Figure 3, the crystallographic form of borates of lithium, potassium, and magnesium at 348 K in the quaternary system are  $\text{Li}_2\text{B}_4\text{O}_7 \cdot 3\text{H}_2\text{O}$ ,  $\text{K}_2\text{B}_4\text{O}_7 \cdot 4\text{H}_2\text{O}$ , and  $\text{MgB}_4\text{O}_7 \cdot 9\text{H}_2\text{O}$ , respectively; their corresponding molecular formulas can be abbreviated to  $\text{Li}_2\text{B}_4\text{O}_7 \cdot 3\text{H}_2\text{O}$ ,  $\text{K}_2\text{B}_4\text{O}_7 \cdot 4\text{H}_2\text{O}$ , and  $\text{MgB}_4\text{O}_7 \cdot 9\text{H}_2\text{O}$ . The invariant point E are constructed with three salts, which are  $\text{Li}_2\text{B}_4\text{O}_7 \cdot 3\text{H}_2\text{O} + \text{K}_2\text{B}_4\text{O}_7 \cdot 4\text{H}_2\text{O} + \text{MgB}_4\text{O}_7 \cdot 9\text{H}_2\text{O}$ .

Table 2 and Figure 1 show that there is no double salt or solid solution formed in the quaternary system at 348 K. The phase diagram (Figure 1) is comprised of one invariant point,

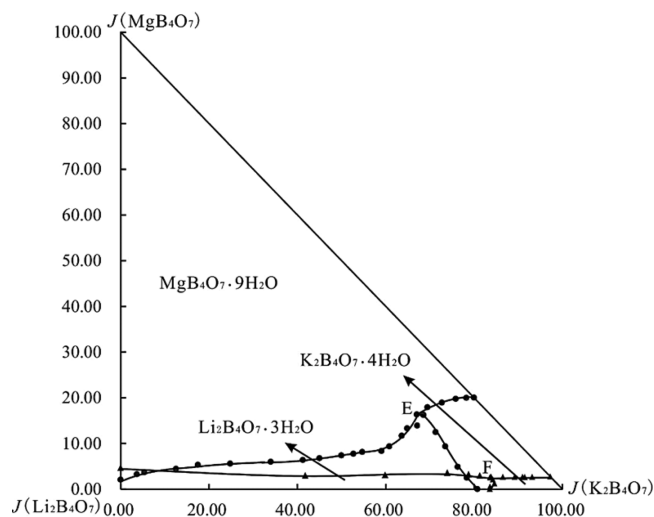


**Figure 2.** Phase diagram of the quaternary system  $\text{Li}^+$ ,  $\text{K}^+$ ,  $\text{Mg}^{2+}$ //borate– $\text{H}_2\text{O}$  at 288 K<sup>14</sup> and 348 K: ●, experimental point at 348 K; ▲, experimental point at 288 K;<sup>14</sup> E, invariant point at 348 K; F, invariant point at 288 K.<sup>14</sup>

three univariant curves, and three crystallization fields. Point E is the invariant point of this quaternary system saturated with three salts. The composition of the equilibrium solution is  $w(\text{K}_2\text{B}_4\text{O}_7) = 40.19\%$ ,  $w(\text{Li}_2\text{B}_4\text{O}_7) = 6.44\%$ ,  $w(\text{MgB}_4\text{O}_7) = 7.31\%$ , and  $w(\text{H}_2\text{O}) = 46.06\%$ . The three crystallization fields correspond to three single salts,  $\text{K}_2\text{B}_4\text{O}_7 \cdot 4\text{H}_2\text{O}$ ,  $\text{Li}_2\text{B}_4\text{O}_7 \cdot 3\text{H}_2\text{O}$ , and  $\text{MgB}_4\text{O}_7 \cdot 9\text{H}_2\text{O}$ . The size of the crystalline area is in the order  $\text{MgB}_4\text{O}_7 \cdot 9\text{H}_2\text{O} > \text{Li}_2\text{B}_4\text{O}_7 \cdot 3\text{H}_2\text{O} > \text{K}_2\text{B}_4\text{O}_7 \cdot 4\text{H}_2\text{O}$ , which shows that the solubility of  $\text{MgB}_4\text{O}_7 \cdot 9\text{H}_2\text{O}$  is the lowest in the system; it means the salt  $\text{MgB}_4\text{O}_7 \cdot 9\text{H}_2\text{O}$  can be more easily separated from the solution than the other coexisting salts at 348 K.

Figure 2 shows the comparisons between the stable phase diagrams at 288 K<sup>14</sup> and 348 K. The crystallization forms of the salts are not changed with the increase of temperature, whereas the crystallization zones of salts have changed. The crystallization zone of  $\text{MgB}_4\text{O}_7 \cdot 9\text{H}_2\text{O}$  decreased at 348 K, while the crystallization zones of  $\text{K}_2\text{B}_4\text{O}_7 \cdot 4\text{H}_2\text{O}$  and  $\text{Li}_2\text{B}_4\text{O}_7 \cdot 3\text{H}_2\text{O}$

$\cdot 3\text{H}_2\text{O}$  are both enlarged, meaning the solubility of  $\text{MgB}_4\text{O}_7 \cdot 9\text{H}_2\text{O}$  increases evidently with the increase of temperature and the decrease of temperature is beneficial to the crystallization of magnesium borate. From Table 2 and Figure 1, it can be seen that the solubility of  $\text{K}_2\text{B}_4\text{O}_7$  is the greatest among the coexisting salts at 348 K; thus, the physicochemical properties are mainly affected by the  $\text{K}_2\text{B}_4\text{O}_7$  content in the equilibrium solution. On account of this, the water content diagram (Figure 4) and the physicochemical properties versus composition

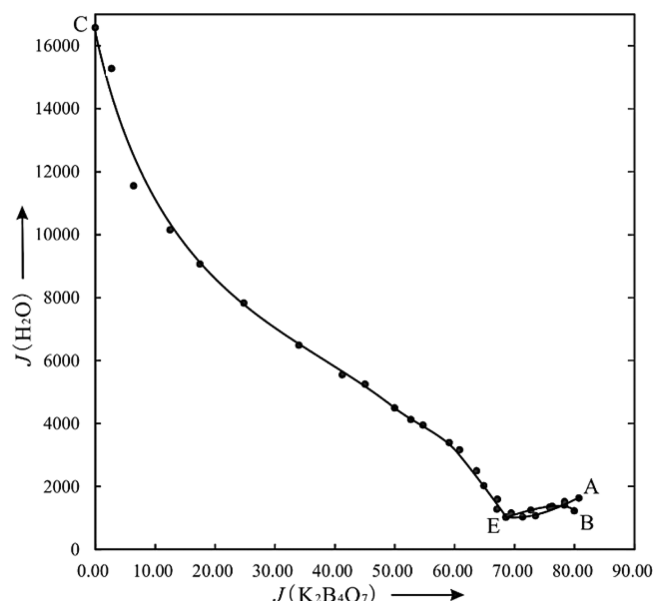


**Figure 4.** Water content diagram of the quaternary system  $\text{Li}^+$ ,  $\text{K}^+$ ,  $\text{Mg}^{2+}$ //borate– $\text{H}_2\text{O}$  at 348 K.

diagrams (Figures 5–7) were plotted with  $J(\text{K}_2\text{B}_4\text{O}_7)$  as abscissa. From Figure 4, it can be seen that the water content increases slightly with the increase of  $J(\text{K}_2\text{B}_4\text{O}_7)$  on the univariant curves EB and EA, while the water contents of univariant curve CE decrease obviously from 16527 to 1019. Figures 5 to 7 respectively are the densities, refractive indices, and pH values versus composition diagrams of the system at

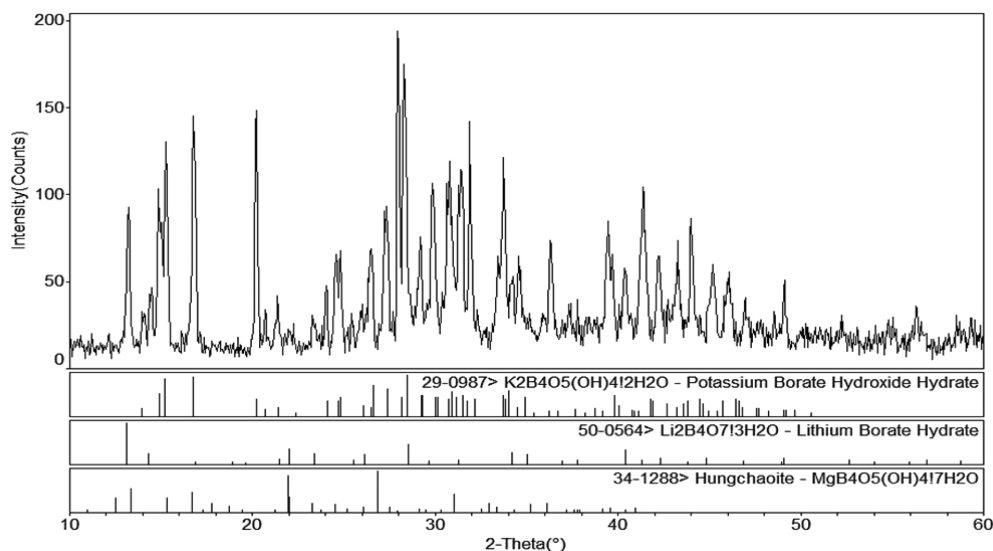


**Figure 3.** X-ray diffraction pattern of the invariant point E ( $\text{Li}_2\text{B}_4\text{O}_7 \cdot 3\text{H}_2\text{O}$ ,  $\text{K}_2\text{B}_4\text{O}_5(\text{OH})_4 \cdot 2\text{H}_2\text{O}$ , and  $\text{MgB}_4\text{O}_5(\text{OH})_4 \cdot 7\text{H}_2\text{O}$ ).



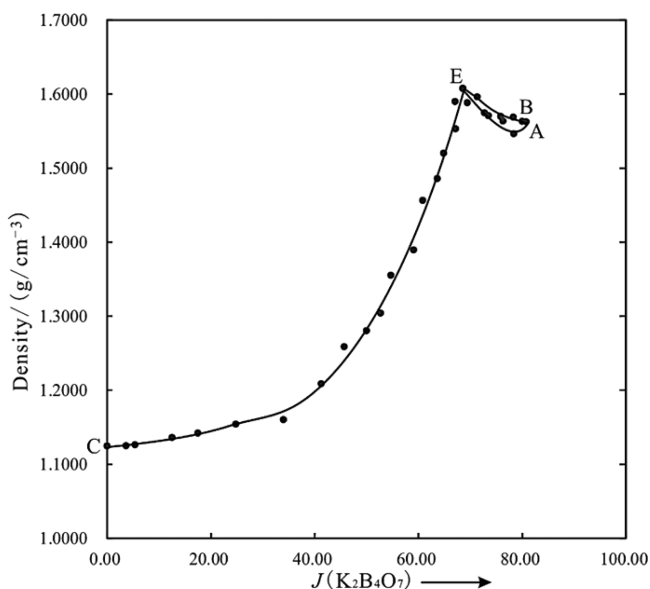


**Figure 5.** Densities vs composition diagram of the quaternary system  $\text{Li}^+$ ,  $\text{K}^+$ ,  $\text{Mg}^{2+}$ //borate- $\text{H}_2\text{O}$  at 348 K.

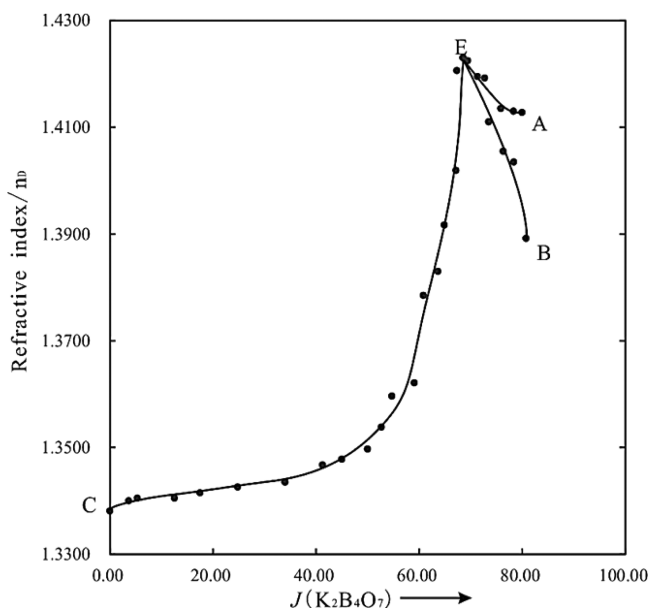


**Figure 6.** Refractive indices vs composition diagram of the quaternary system  $\text{Li}^+$ ,  $\text{K}^+$ ,  $\text{Mg}^{2+}$ //borate- $\text{H}_2\text{O}$  at 348 K.

348 K. With the increasing of  $J(\text{K}_2\text{B}_4\text{O}_7)$ , the densities and refractive indices both increase on the univariant curve CE, while decreasing on the univariant curve EB and EA and reaching the maximum at invariant point E. It can be observed from Figure 7 that on the univariant curves CE and EA, the pH values of the solution increase with the increasing of  $J(\text{K}_2\text{B}_4\text{O}_7)$ , while, on the univariant curve EB, the pH values have a different trend.

## CONCLUSION

Stable phase equilibrium of the aqueous quaternary system  $\text{Li}^+$ ,  $\text{K}^+$ ,  $\text{Mg}^{2+}$ //borate- $\text{H}_2\text{O}$  was investigated at 348 K using an isothermal dissolution method. According to the experimental data, the phase diagram and corresponding physicochemical properties vs composition diagrams were plotted. Results show

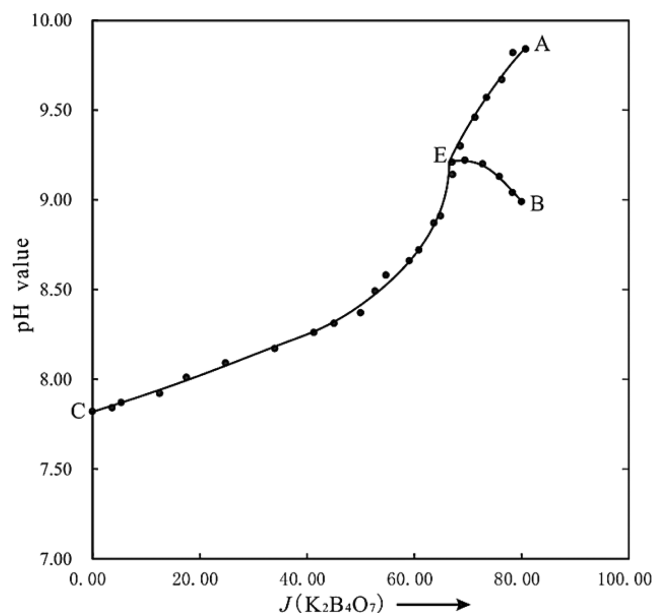


**Figure 7.** pH values vs composition diagram of the quaternary system  $\text{Li}^+$ ,  $\text{K}^+$ ,  $\text{Mg}^{2+}$ //borate- $\text{H}_2\text{O}$  at 348 K.

that the quaternary system is of a simple type, neither solid solutions nor double salts formed at 348 K. The stable phase diagram of the quaternary system composed of one invariant point, three univariant curves, and three crystalline phase regions. Based on the comparisons between the stable phase diagrams at 288 K and 348 K, the crystallization form of the salts is not changed with the increase of temperature, whereas the scopes of the crystallization regions are obviously changed. With the increase of  $J(\text{K}_2\text{B}_4\text{O}_7)$ , the water contents decrease obviously from 16527 to 1019, and the physicochemical property values increase obviously on the univariant curve CE. While on the univariant curves EB and EA, the water content increases with the increase of  $J(\text{K}_2\text{B}_4\text{O}_7)$ , and the densities and refractive indices decrease slightly with the increase of  $J(\text{K}_2\text{B}_4\text{O}_7)$ .

## AUTHOR INFORMATION

### Corresponding Author

\*E-mail: zengy@cdut.edu.cn. Tel.: 86-28-84079016. Fax: 86-28-84079074.

### Funding

This research was supported by the National Natural Science Foundation (Grants 41173071 and 41473059) and Key Foundation (Grant 41030426) of China, the National High Technology Research and Development Program of China (Grant 2012AA061704), the Research Fund for the Doctoral Program of Higher Education from the Ministry of Education of China (Grant 20115122110001), the Sichuan youth science and technology innovation research team funding scheme (Grant 2013TD0005), and the Innovation Team of Chengdu University of Technology (Grant KYTD201405).

### Notes

The authors declare no competing financial interest.

## REFERENCES

- (1) Lin, Y. T.; He, J. Q.; Wang, T. D.; Ye, M. C. Geochemical Characteristics of Potassium-Rich Brine in Middle Triassic Chengdu

Salt Basin of Sichuan Basin and Its Prospects for Brine Tapping. *Geol. Chem. Miner.* **2002**, *24*, 72–84.

(2) Yu, S. S.; Tan, H. B.; Liu, X. Q.; Cao, G. C. *The sustainable utilization researches of Qarhan salt lake resource*; Science Press: Beijing, 2009.

(3) Vine, J. D. Lithium resources and requirements by the year 2000. *Geological survey professional paper 1005*; United States Government Printing office: Washington, DC, USA, 1976.

(4) Lin, Y. T.; Tang, Q. Distribution of Brine in Sichuan Basin and Its Prospects for Tapping. *Geol. Chem. Miner.* **1999**, *21*, 209–214.

(5) Zheng, M. P.; Yuan, H. R.; Zhang, Y. S.; Liu, X. F.; Chen, W. X.; Li, J. S. Regional Distribution and Prospects of Potash in China. *Acta Geol. Sin. (Engl. Ed.)* **2010**, *84*, 1523–1553.

(6) Li, W.; Dong, Y. P.; Song, P. S. *The development and Utilization of Salt Lake Brine Resource*; Chemical Industry Press: Beijing, China, 2012.

(7) Yu, X. D.; Zeng, Y.; Yao, H. X.; Yang, J. Y. Metastable Phase Equilibria in the Aqueous Ternary Systems  $\text{KCl} + \text{MgCl}_2 + \text{H}_2\text{O}$  and  $\text{KCl} + \text{RbCl} + \text{H}_2\text{O}$  at 298.15 K. *J. Chem. Eng. Data* **2011**, *56*, 3384–3391.

(8) Yu, X. D.; Zeng, Y. Metastable Phase Equilibria in the Aqueous Ternary Systems  $\text{KCl} + \text{MgCl}_2 + \text{H}_2\text{O}$  and  $\text{KCl} + \text{RbCl} + \text{H}_2\text{O}$  at 323.15 K. *J. Chem. Eng. Data* **2010**, *55*, 5771–5776.

(9) Yu, X. D.; Zeng, Y.; Yin, Q. H.; Mu, P. T. Solubilities, Densities, and Refractive Indices of the Ternary Systems  $\text{KCl} + \text{RbCl} + \text{H}_2\text{O}$  and  $\text{KCl} + \text{MgCl}_2 + \text{H}_2\text{O}$  at 348.15 K. *J. Chem. Eng. Data* **2012**, *57*, 3658–3663.

(10) Yu, X. D.; Zeng, Y.; Yang, J. Y. Solid Liquid Isothermal Evaporation Metastable Phase Equilibria in the Aqueous Quaternary System  $\text{LiCl} + \text{KCl} + \text{RbCl} + \text{H}_2\text{O}$  at 298.15 K. *J. Chem. Eng. Data* **2012**, *57*, 127–132.

(11) Li, Z. Q.; Yu, X. D.; Yin, Q. H.; Zeng, Y. Thermodynamics Metastable Phase Equilibria of Aqueous Quaternary System  $\text{LiCl} + \text{KCl} + \text{RbCl} + \text{H}_2\text{O}$  at 323.15 K. *Fluid Phase Equilib.* **2013**, *358*, 131–136.

(12) Yin, Q. H.; Zeng, Y.; Yu, X. D.; Mu, P. T.; Tan, Q. Metastable Phase Equilibrium in the Quaternary System  $\text{LiCl} + \text{KCl} + \text{RbCl} + \text{H}_2\text{O}$  at 348.15 K. *J. Chem. Eng. Data* **2013**, *58*, 2875–2880.

(13) Yu, X. D.; Yin, Q. H.; Jiang, D. B.; Zeng, Y. Metastable Equilibrium for the Quaternary System Containing with Lithium + Potassium + Magnesium + Chloride in Aqueous Solution at 323K. *Korean J. Chem. Eng.* **2014**, *31*, 1065–1069.

(14) Xiao, L. J.; Sang, S. H.; Zhao, X. P. Study on Phase Equilibrium of the Quaternary System  $\text{K}_2\text{B}_4\text{O}_7 + \text{Li}_2\text{B}_4\text{O}_7 + \text{MgB}_4\text{O}_7 - \text{H}_2\text{O}$  at 288 K. *J. Salt Chem. Ind.* **2010**, *39*, 18–20.

(15) Zhang, Y. J.; Zeng, Y.; Yu, X. D. Study on Phase Equilibrium of Ternary System  $\text{Li}^+, \text{K}^+//\text{Borate} - \text{H}_2\text{O}$  at 348 K. *Inorg. Chem. Ind.* **2013**, *45*, 15–17.

(16) Jin, J.; Zeng, Y.; Yu, X. D.; Tan, Q. Stable Phase Equilibrium of the Ternary System  $\text{K}^+, \text{Mg}^{2+}//\text{B}_4\text{O}_7^{2-} - \text{H}_2\text{O}$  at 348 K. *J. Mineral. Petrol.* **2013**, *33*, 116–120.

(17) Jing, Y. A new synthesis method for magnesium borate. *Sea-Lake Salt Chem. Ind.* **2000**, *29*, 24–25.

(18) Institute of Qinghai Salt-Lake of Chinese Academy of Sciences. *Analytical Methods of Brines and Salts*, 2nd ed.; Chinese Science Press: Beijing, China, 1984.

(19) Yin, Q. H.; Mu, P. T.; Tan, Q.; Yu, X. D.; Li, Z. Q.; Zeng, Y. Phase Equilibria for the Aqueous Reciprocal Quaternary System  $\text{Rb}^+, \text{Mg}^{2+} // \text{Cl}^-, \text{Borate-H}_2\text{O}$  at 348 K. *J. Chem. Eng. Data* **2014**, *59*, 2235–2241.